



# Characteristics and mechanisms of large-scale old landslides and landslide dams in the Loess Plateau—A case study from Daning County, Shanxi Province, China

Zhenming Zhao<sup>a</sup>, Yaming Tang<sup>a,b,\*</sup>, Fan Feng<sup>a</sup>, Zhengguo Li<sup>a</sup>, Yong Xu<sup>a</sup>, Bo Hong<sup>a</sup>, Wei Feng<sup>a</sup>

<sup>a</sup> Xi'an Center of China Geological Survey, Xi'an, 710119, China

<sup>b</sup> Institute of Earth Environment, Chinese Academy of Sciences, Xi'an, 710061, China

## ARTICLE INFO

### Keywords:

Old landslide  
Landslide dam  
Deposit  
Carbon-14 dating  
Mechanism  
Loess Plateau

## ABSTRACT

Giant landslides and dammed lakes occurred frequently during the prehistoric period; however, their mechanisms often remain an open issue because they are complex. This study used field investigations to observe four old landslides and three landslide dams in Daning County, Shanxi Province, China. Remote sensing images captured during different periods were used to compare the landforms of landslides, landslide dams, and their surrounding environments in detail. Subsequently, their shapes, scales, spatial distributions, and positional relationships were determined. The ages of <sup>14</sup>C obtained from the paleolandslide dam lake (PDL) deposits were  $3742 \pm 95$ ,  $4115 \pm 121$ ,  $6544 \pm 91$ ,  $7814 \pm 109$  cal a BP. The <sup>14</sup>C ages of the deposits under the sliding surfaces of the old landslides were  $2748 \pm 27$ ,  $4470 \pm 54$ , and  $8245 \pm 79$  cal a BP. Based on the actual physical geographical conditions and geomorphological characteristics of the region, combined with the above age data, that the following conclusions were made: (i) During the Holocene, from 2700 to 8200 years ago, heavy rainfall was the main reason for the occurrence of landslides and landslide dams in the region. (ii) Under the condition of heavy rainfall, the slopes with angles  $>60^\circ$  in the Loess Plateau are prone to form landslide masses, and the size of the landslide is related to rainfall intensity. A landslide dam was easily formed when the sliding direction was perpendicular to the direction of the valley. It is difficult to form landslide dams when the sliding direction is almost consistent with the downward direction of the valley. (iii) The formation mechanism of old landslides shows that collapse or sliding may occur suddenly in loess geological masses under an external rainfall scenario. Moreover, the process of landslide dams is related to the geomorphic forms of the original valley.

## 1. Introduction

Landslides have been one of the most frequent natural hazards worldwide since the prehistoric period [1–3]. Among landslide-prone areas worldwide, the Loess Plateau is famous for its complex landforms and frequent human engineering activities. Geological disasters in the region cause serious casualties and property loss annually [4–7]. Factors that induce landslides on the Loess

\* Corresponding author. Xi'an Center of China Geological Survey, Xi'an, 710119, China.  
E-mail address: [tyaming@mail.cgs.gov.cn](mailto:tyaming@mail.cgs.gov.cn) (Y. Tang).

<https://doi.org/10.1016/j.heliyon.2023.e19910>

Received 15 April 2023; Received in revised form 5 September 2023; Accepted 5 September 2023

Available online 6 September 2023

2405-8440/© 2023 The Authors. Published by Elsevier Ltd. This is an open access article under the CC BY-NC-ND license (<http://creativecommons.org/licenses/by-nc-nd/4.0/>).

Plateau include rainfall [8], human engineering activities [9], earthquakes [10], and irrigation [11]. Among these, short-term heavy rainfall or long-term continuous rainfall causes redistribution of slope gravity and stress fields to form landslides, which is the most common situation and has a strong relationship with the collapsibility of loess itself. Therefore, it is essential to strengthen the investigation of geological disasters in the Loess Plateau and analyze the formation mechanism to reduce the risk of landslide disasters [12,13].

In recent years, research on landslides in the Loess Plateau has mainly focused on the distribution of landslides [14], investigation and analysis of individual landslides [15,16], physical property tests of loess [17], landslide susceptibility, and risk assessment [18, 19]. However, the aforementioned research has rarely involved the formation of ancient landslides and landslide dams on the Loess Plateau. During geological history, the East Asian monsoon and changes in precipitation have induced a series of ancient landslides and landslide dams on the Loess Plateau [20–22]. These landslides may be activated by current and future extreme rainfall conditions [23–26]. Therefore, it is important to investigate and analyze landslides and landslide dams. Recently, the China Geological Survey found and confirmed several landslides of different ages and scales and dammed lake sites beneath the landslides within 13 km<sup>2</sup> of Daning County, Shaanxi Province, in a geological hazard survey of the Lvliang Mountains in China. Samples were taken from the paleolandslide dam lake (PDL) deposits of the landslide dams formed by 1, 2, and 3# landslide masses, and their ages were 3700, 4100, and 7800 cal a BP, respectively. Then, the deposit samples were taken under the sliding surface of 1# and 4# landslide masses, and the ages of 4400 and 8200 cal a BP were obtained, respectively. Furthermore, in the valley to the east of Mingti Village in Daning County, a huge landslide mass and a dammed lake site were found, with a total earthwork of  $1.2 \times 10^7$  m<sup>3</sup>, and the surface area of the landslide dam reached  $5.0 \times 10^4$  m<sup>2</sup>. The bottom deposits of the landslide dam were sampled, and their ages were found to be 6500 cal a BP. Based on the geographical location and geomorphic characteristics of the landslide dam, combined with remote sensing images and carbon 14 (<sup>14</sup>C) dating data of the landslide dam deposits, this study discusses the formation process of the landslide and its relationship with historical heavy rainfall and offers suggestions for disaster management in this area.

## 2. Study area and methods

### 2.1. Summary for the study area

Daning County is located to the west of Linfen City, Shanxi Province, China, at the southern end of the Lvliang Mountains (Fig. 1). Its geographical coordinates are 110°28'01"–111°00'43"E , 36°16'24"–36°36'55"N, with a north-south length of 34 km, an east-west width of 38 km, and a total area of approximately 966.8 km<sup>2</sup>. The elevation in the area ranges from 485 to 1715 m above sea

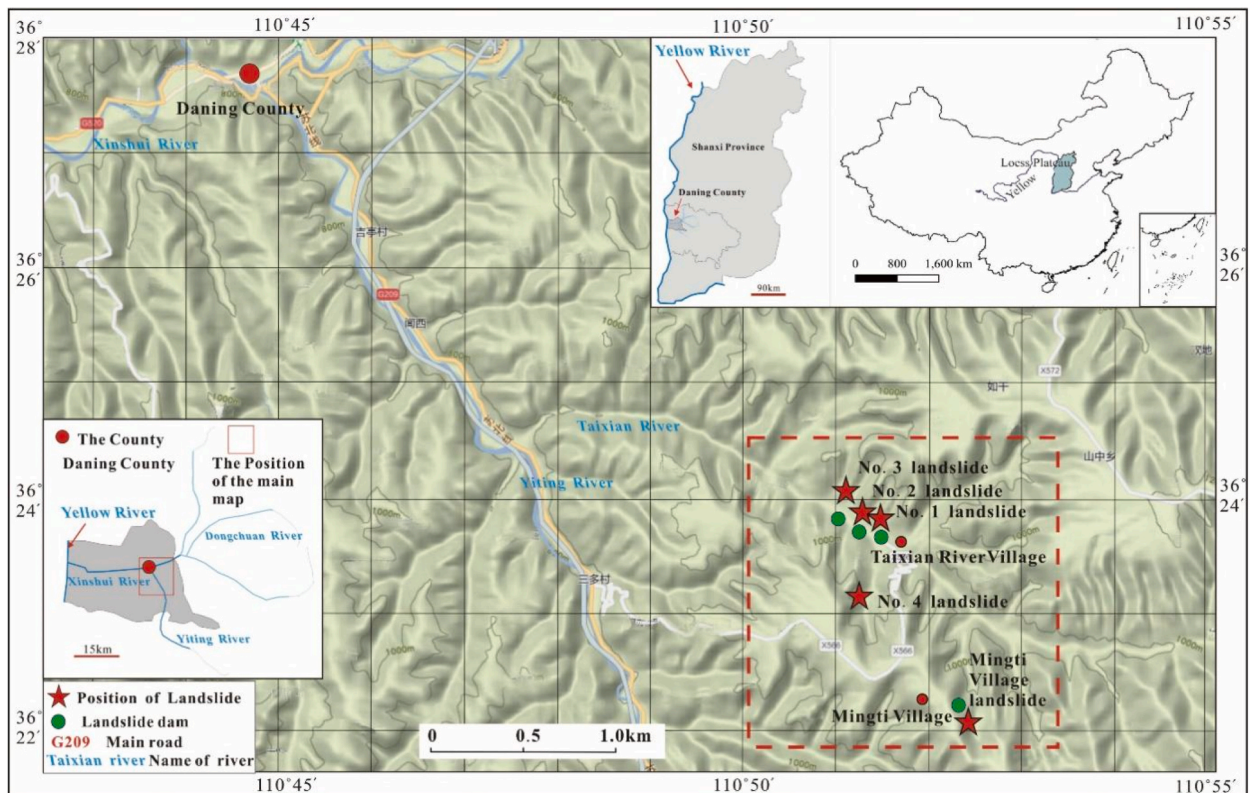


Fig. 1. Location of the study area and observed old landslides and landslide dams.

level, with the terrain being higher in the northern and southern parts, lower in the middle, and higher in the eastern part than in the western part. The topography is dominated by loess hills and gullies. The eastern part belongs to the mountainous region of the Lvliang Mountains, and the loess hills are more important in the northern and southern parts. Geologically, the region is characterized by Cambrian–Jurassic sedimentary rocks and Quaternary deposits. In particular, sandstone, mudstone, sandy mudstone, and Quaternary loess strata are extensive outcrops [18].

Regarding the climate regime, the study area has a semi-arid continental monsoon climate in a warm temperate zone, with four distinct seasons. It is hot and rainy in summer and cold and dry in winter. The average annual precipitation is approximately 470 mm, and rainfall is concentrated in June, September, and July.

Located in the middle of the Loess Plateau, this area is frequently affected by landslide disasters owing to the special characteristics of loess, including collapsibility and water sensitivity [6,8]. From October 2 to 7, 2021, the strongest autumn rainfall occurred in Shanxi Province since the meteorological records, with an average rainfall of 119 mm and a maximum rainfall of 285.2 mm. Heavy rainfall has affected 1.8 million people in Shanxi Province and triggered multiple geological disasters in the entire region, resulting in 15 deaths and 3 disappearances, with a direct economic loss of 230 million RMB.

## 2.2. Methods

### 2.2.1. Field survey

To determine the regularity and formation mechanism of geological disasters in the Lvliang Mountains area, a group of ancient landslides, including four landslides, namely 1#, 2#, 3#, and 4# landslide (Fig. 1), were identified through field surveys in the Taixian River catchment in Daning County. Another large-scale ancient landslide occurred in Mingti village, 1.5 km away from the landslide

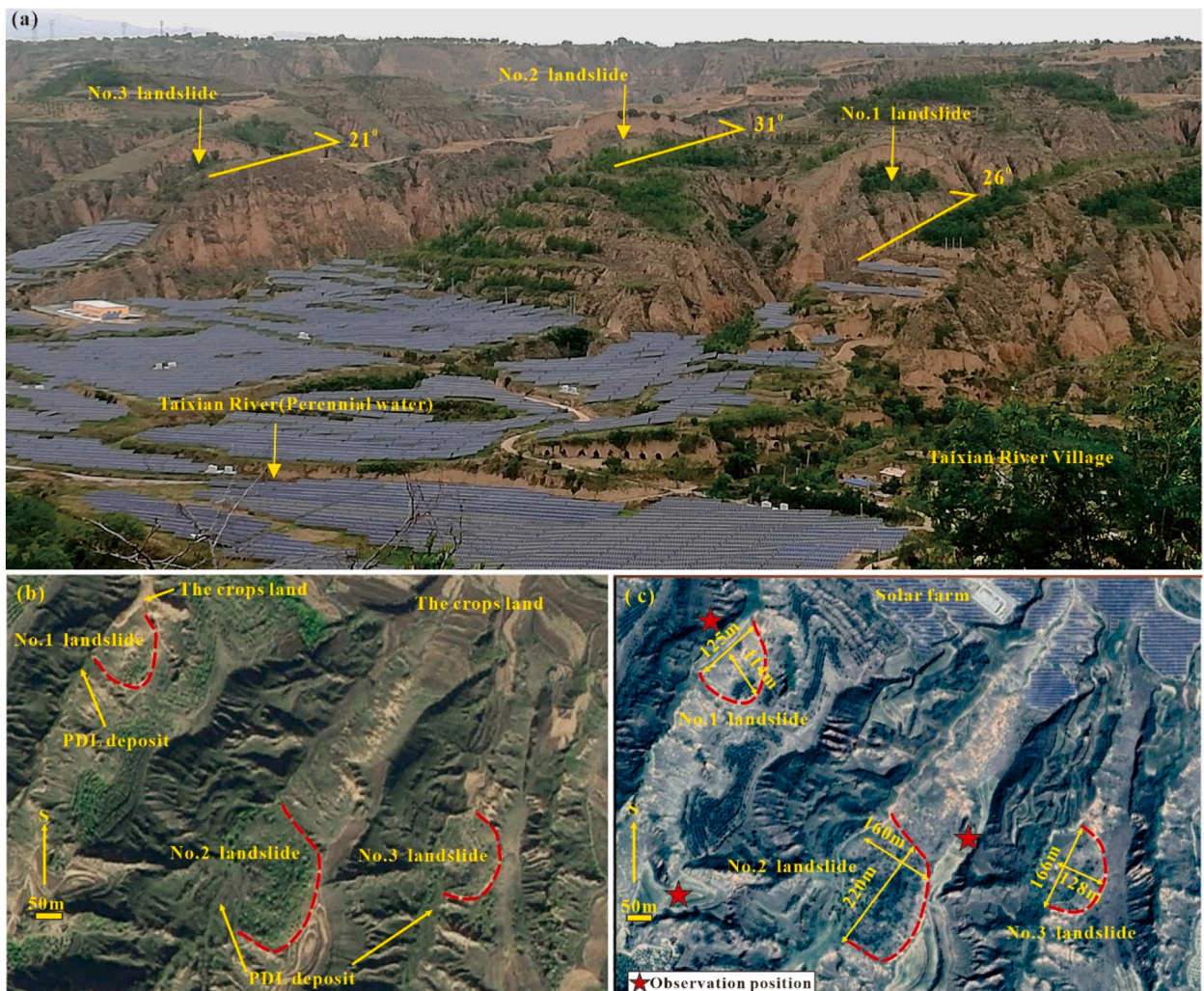


**Fig. 2.** The photo and remote sensing images of the Taixianhe 1–3# landslides: (a) photos taken in the field, (b) remote sensing images from 2005, and (c) remote sensing images from 2020.

group, which was named Mingti landslide.

The basic characteristics of the ancient landslide group and landslide dams were obtained using measurements with a laser range finder, drone, and long tape. Drilling and trial trenching were also conducted to expose the internal characteristics of the old landslides and landslide dams. Geological data, soil characteristics, landslide bodies, and sliding surfaces have been revealed using these methods.

### 2.2.2. Remote sensing

Remote-sensing imaging technology plays an important role in the investigation of natural disasters [27], particularly geological disasters. Remote sensing technology is used to collect electromagnetic signals far from the ground to obtain a wide range of ground information, enabling researchers to understand the ground situation more comprehensively. In this study, remote sensing images captured during different periods were used to interpret landslides in detail, in combination with actual measurements. The remote sensing images used in this study were sourced from the GF-1 and GF-2 satellites and Google Earth (<https://earth.google.com/web/>). The former two are commercial products with 8-m resolution and four bands (RGB + near-infrared bands), and the latter is open-source. Site photos (Fig. 2 (a)) and multi-period remote sensing images from 2005 (Fig. 2 (b)) and 2020 (Fig. 2 (c)) of the final ancient landslide group are shown in Fig. 2.

### 2.2.3. Carbon-14 dating

$^{14}\text{C}$  dating is a method for measuring residual radioactive energy, because animals and plants absorb  $^{14}\text{C}$  from carbon dioxide throughout their lives. Once they die, they immediately stop the carbon exchange with the biosphere. The  $^{14}\text{C}$  content began to decrease, and the rate of reduction is determined by radioactive decay. By knowing the residual  $^{14}\text{C}$  content in the sample, we can determine the age of death of the organic matter. This technology can be applied to natural hazards to identify the age of ancient events and their behavior in certain aspects [15,28–31].

This study collected samples from the PDL deposits of the landslide dam and deposits below the sliding surface of the landslide, and  $^{14}\text{C}$  ages were obtained through testing. The samples for landslide dams were normally collected from the bottom of the PDL deposit, and those for old landslides were collected near the toe of the landslides to ensure accurate age results of the materials. The depths and materials of the PDL deposits were determined primarily using drills and trial trenches. Detailed information on the collected samples is as follows.

The sample from the Taixianhe 1# landslide dam was collected 110 cm below the dam. The  $^{14}\text{C}$  dating sample number was 529H101, and the sampling coordinate was  $\text{N}36^{\circ}24'0.99''$ ,  $\text{E}110^{\circ}51'48.97''$ . Sample 530H102 was collected under the sliding surface of the landslide and its coordinates were similar to those of the landslide dam sample.

The sample for the Taixianhe 2# landslide dam was collected 120 cm below the dam. The  $^{14}\text{C}$  dating sample number was 530H201,



Fig. 3. The photo of the Taixianhe 4# landslide, and sampling locations of deposits.

and the sampling coordinate was  $N36^{\circ}24'15.71''$ ,  $E110^{\circ}51'40.40''$ . For the landslide sample, a slope with an angle of  $60^{\circ}$  and a depth of 70 cm was excavated near the toe. The  $^{14}\text{C}$  age sample (530H202) was collected at the coordinate of  $N36^{\circ}24'12.90''$ ,  $E110^{\circ}51'31.13''$ .

For the Taixianhe 3# landslide dam, a sample was collected from a PDL deposit 120 cm below the dam. The sampling (601H301) coordinate was  $N36^{\circ}24'16.11''$ ,  $E110^{\circ}51'22.70''$ . The slope at the bottom of the sliding surface was excavated to a diameter of 50 cm and a depth of 120 cm. The  $^{14}\text{C}$  age sample 601H302 was collected at the coordinate of  $N36^{\circ}24'10.91''$ ,  $E110^{\circ}51'17.25''$ .

There was no landslide dam for the Taixianhe 4# landslide; therefore, its  $^{14}\text{C}$  sample was collected from the deposit at the bottom of the sliding surface of the landslide (Fig. 3). The sampling (603H401) coordinate was  $N36^{\circ}23'15.79''$ ,  $E110^{\circ}51'30.95''$ . Additionally, sample 603H402 was collected from the collapsed geomorphic deposits on the right side of the sliding surface. The sampling coordinate was  $N36^{\circ}23'20.28''$ ,  $E110^{\circ}51'37.05''$ .

The sample (604H501) for the PDL deposit of the Mingti landslide dam was located in the middle of the landslide dam. The sampling coordinate was  $N36^{\circ}21'46.78''$ ,  $E110^{\circ}52'5068''$ . The other sample, 604H502, with the coordinates  $N36^{\circ}22'06.67''$ ,  $E110^{\circ}52'56.81''$ , was the loose deposit at the bottom of the sliding surface.

The samples were tested at BETA Analytics in Miami, FL, USA. The testing process was performed in strict accordance with the ISO/IEC 17025:2005 standards. The test, modern, and blank samples underwent the same chemical treatment by professional testers and analyzed using an accelerator mass spectrometer.

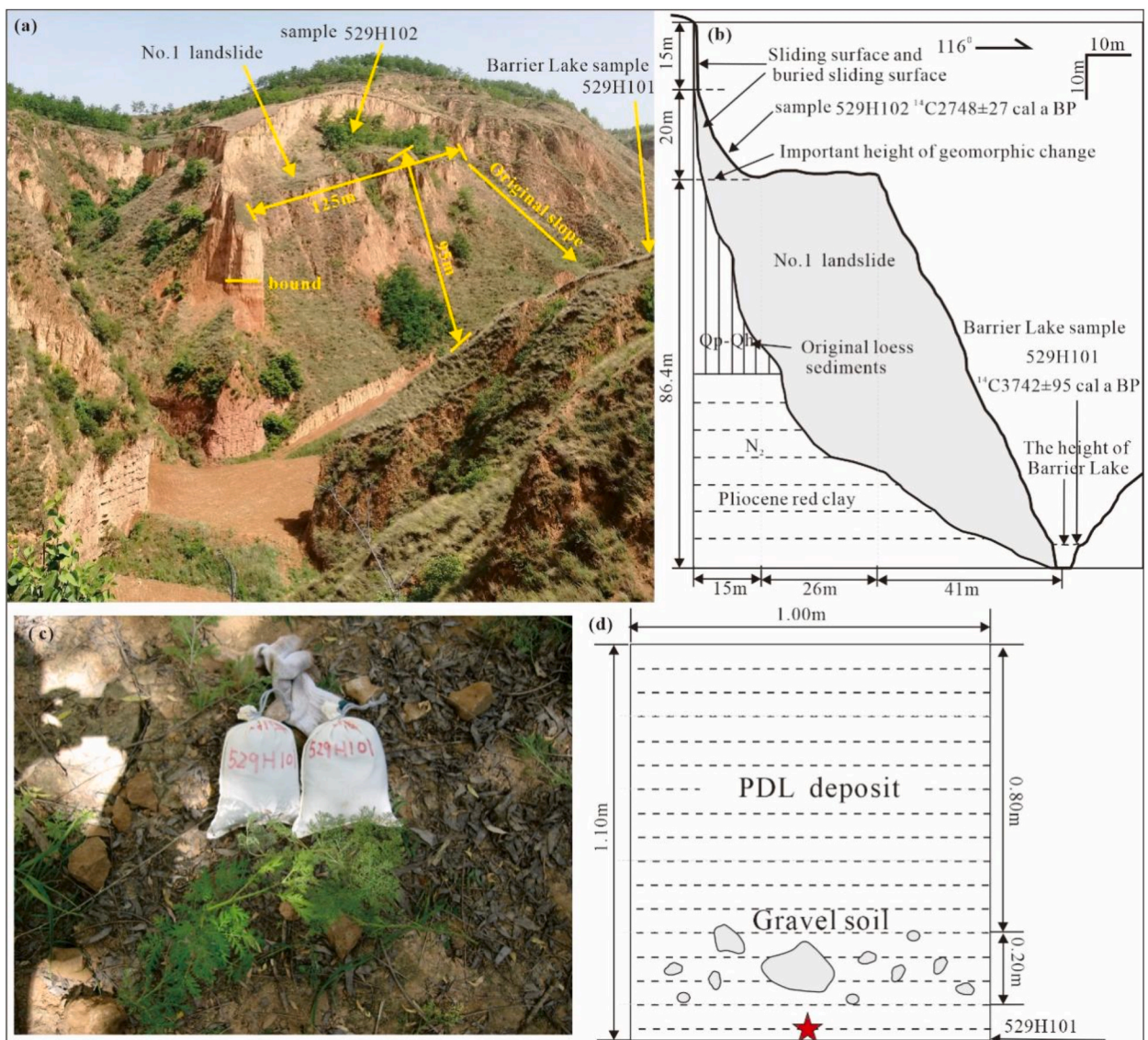


Fig. 4. The basic characteristics of the Taixianhe 1# landslide: (a) the photo taken in the field survey, (b) the profile of the landslide, (c) the photo of the sample, (d) the profile of the PDL deposit.

### 3. Basic characteristics of old landslides and landslide dams

#### 3.1. Basic characteristics of old landslides

A photograph, plan, and profile of Taixianhe 1# landslide mass are shown in Fig. 4, including the photo of the landslide (Fig. 4 (a)), the profile of the landslide (Fig. 4 (b)), the photo of the sample (Fig. 4 (c)), and the profile of the PDL deposit (Fig. 4 (d)). The gully where the landslide mass is located is 26° upward. The horizontal distances between the edge of the landslide mass and the gully are 125, 143, and 28 m from the edge to the bottom of the slope of the sliding surface and 95 m from the edge to the ditch. The slope angle of the landslide mass surface, that is, the slope angle of the original landslide mass without formation, is 65°. The dip angle of the sliding surface is approximately 90° and its height is 15 m. The slightly inclined surface at the bottom of the sliding surface is 15–20 m high. The total volume of the landslide mass is approximately  $32 \times 10^4 \text{ m}^3$ .

The basic characteristics and photos of the Taixianhe 2# landslide are shown in Fig. 5, including the photo of the landslide (Fig. 5 (a)), the photo of the sample (Fig. 5 (b)), the profile of the landslide (Fig. 5 (c)), and the profile of the PDL deposit (Fig. 5 (d)). The direction of the gully where the Taixianhe 2# landslide mass is located is 31°. The horizontal distance of the upper edge of the landslide mass exceeds 209 m, the vertical height, including the sliding surface, is 150 m, and the width of the landslide mass is 220 m. The slope angle from the change point of the landslide surface landform to the bottom of the sliding surface is 30°, and the horizontal distance is 140 m. The length of the front edge near the horizontal surface of the landslide mass is 39 m, and the slope from the front edge to the trench bottom is 54 m long with a slope angle of 60°. The boundary on either side of the landslide mass is clear, and a special landform formed at the bottom of the ditch. The slope angle of the sliding surface is approximately 90° and its height is 30 m. There is no

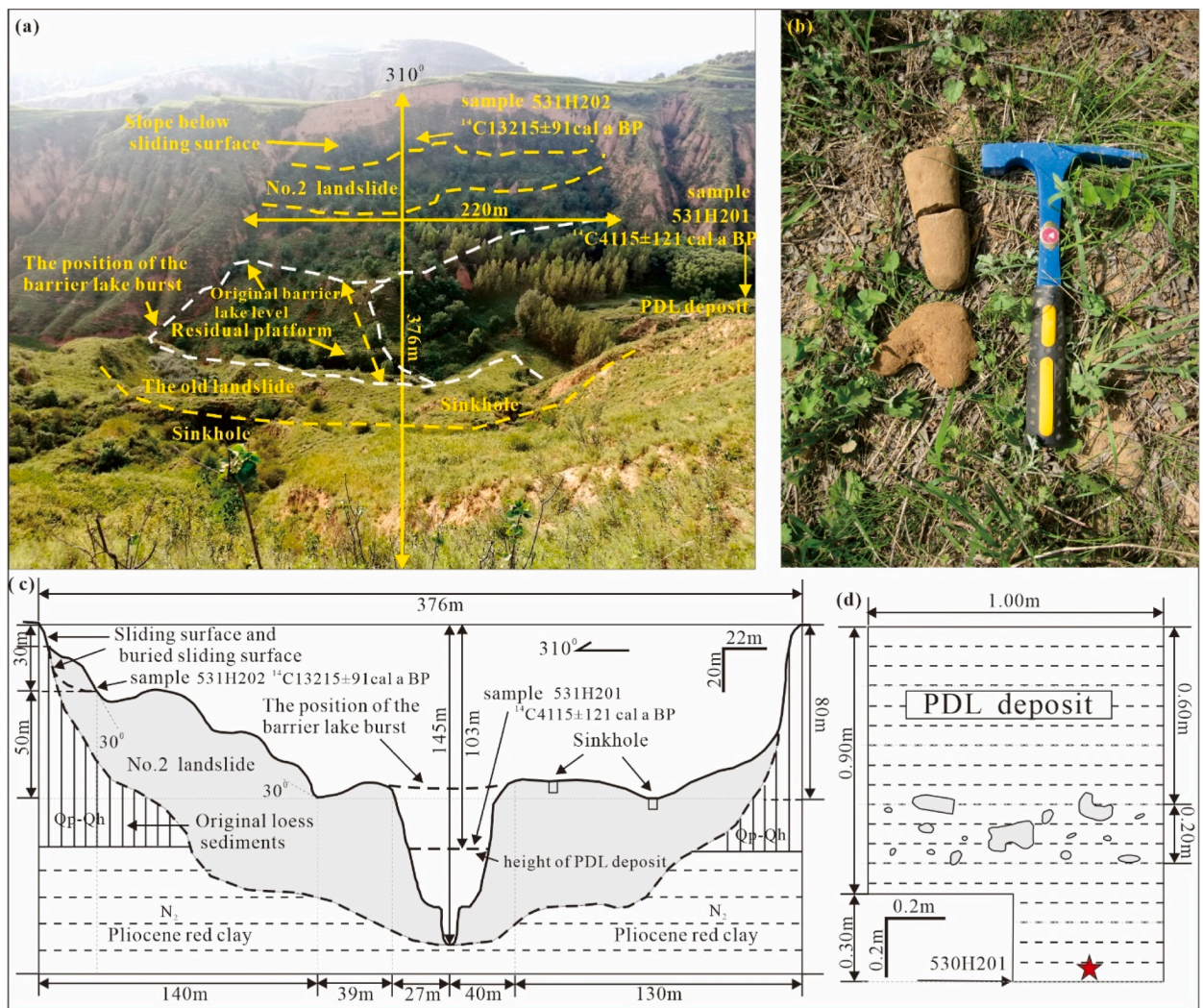


Fig. 5. The basic characteristics of the Taixianhe 2# landslide: (a) the photo taken in the field survey, (b) the photo of the sample, (c) the profile of the landslide, (d) the profile of the PDL deposit.

vegetation on the sliding surface, and the slope angle of the small slope at the bottom of the sliding surface is 60°. The total volume of the landslide mass is approximately  $1.9 \times 10^6 \text{ m}^3$ .

The information of the Taixianhe 3# landslide determined in the field survey included the photo of the landslide overview (Fig. 6 (a)), the sampling process (Fig. 6 (b)), the profile of the landslide (Fig. 6 (c)), and the profile of the PDL deposit (Fig. 6 (d)). The direction of the gully where Taixianhe 3# landslide is located is 21°. The edge of the landslide mass is 166 m wide, 51 m from the edge to the bottom of the sliding surface, 125 m from the edge to the trench obliquely, and the slope angle of the landslide mass is 65°–70°. The surface of the landslide mass has modern gullies and vegetation has developed. The slope angle of the sliding surface is 85°, its height is 11 m, and minimal vegetation is found on the sliding surface. The total volume of the landslide mass is approximately  $1 \times 10^6 \text{ m}^3$ .

The overview and basic characteristics of the Taixianhe 4# landslide were shown in Fig. 7, including the photo when sampling (Fig. 7 (a)), the digging hole during sampling (Fig. 7 (b)), the calcareous tuberculosis of the sampling (Fig. 7 (c)), the location of the sample 603H401 (Fig. 7 (d)), the photo taken when sampling in the field (Fig. 7 (e)), and the location of the sample 604H501 (Fig. 7 (f)). The Taixianhe 4# landslide mass is located at the mouth of the Taixian River, with a sliding direction of 95°. The occurrence of sliding surface is 95°∠80° and the height is 75 m. The width of the landslide mass is 190 m, and the distance from the bottom of the sliding surface to the front edge of the landslide mass surface is 387 m. The total volume of the landslide mass is approximately  $260 \times 10^4 \text{ m}^3$ .

The Mingti landslide mass (Fig. 8) is located in a valley on the northeastern side of Mingti Village, Sanduo Township, Daning County. The extension direction of the gully is 10° and a landslide mass appears on the east side of the gully, with a sliding direction of 280°, which completely blocks the flow direction of the gully. The landslide mass has an evident seat shape. Vegetation has developed on the sliding surface, and the scratch of the original sliding is slightly visible. The occurrence of the sliding surface is 280°∠70° and the slope angle is steep. According to the actual measurements (Fig. 8 (a)) and remote sensing stereo image interpretation (Fig. 8 (b)) of the landslide mass, the sliding direction of the landslide mass is 570 m long, the width of both sides is 597 m, and the height of the sliding

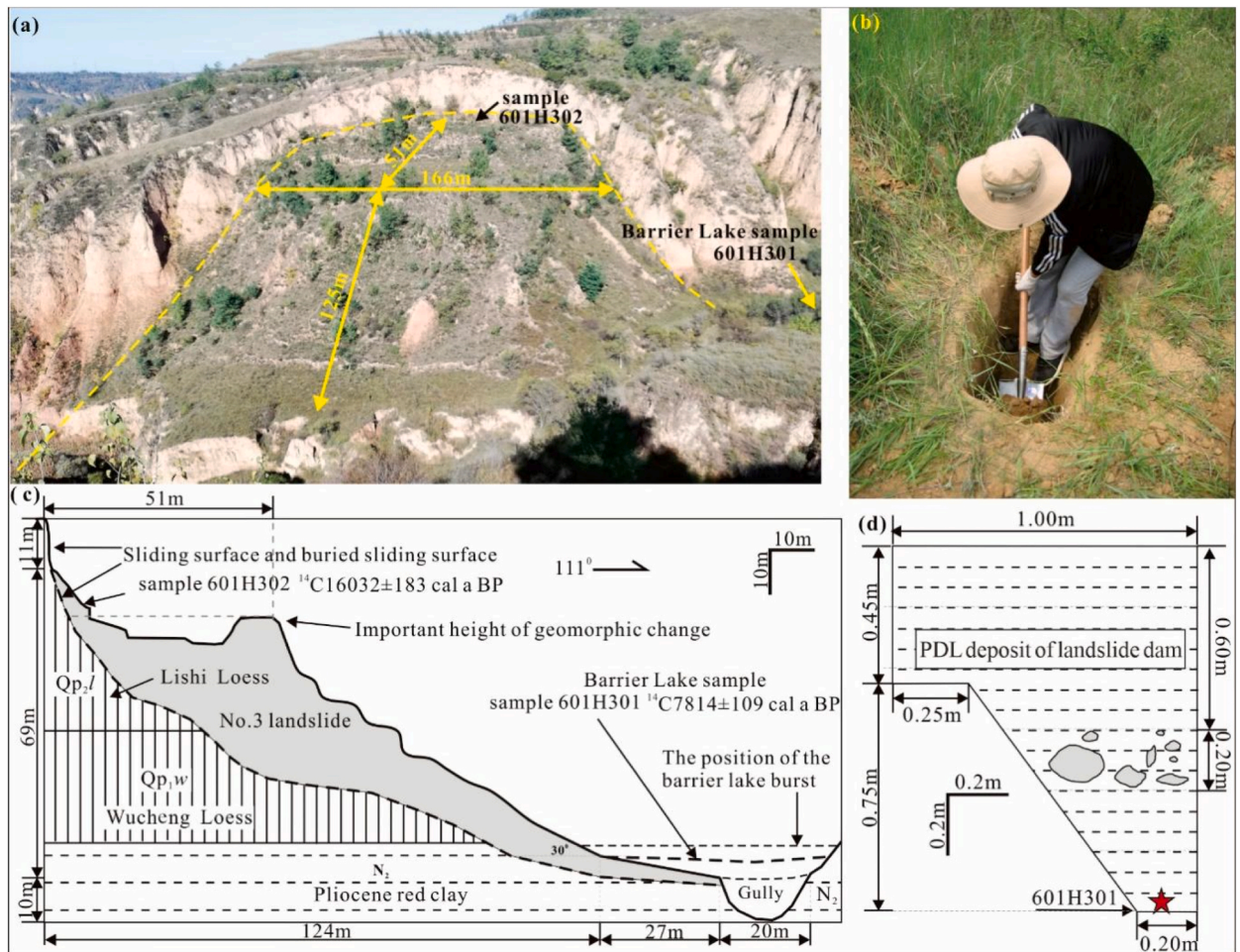
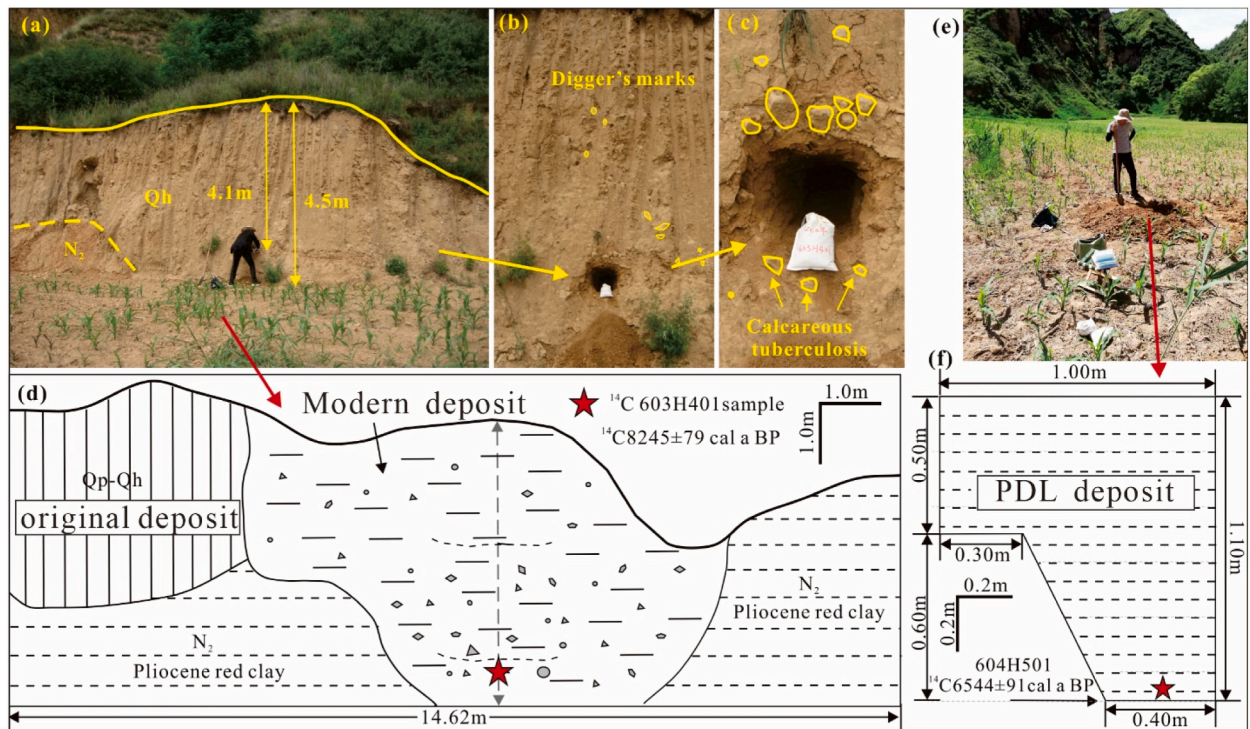


Fig. 6. The basic characteristics of the Taixianhe 3# landslide: (a) the photo taken in the field survey, (b) the sampling process, (c) the profile of the landslide, (d) the profile of the PDL deposit.



**Fig. 7.** The basic characteristics of the Taixianhe 4# landslide: (a) the photo showing the overview when sampling, (b) the digging hole during sampling, (c) the calcareous tuberculosis of the sampling, (d) the location of the sample 603H401, (e) the photo taken when sampling in the field, (f) the location of the sample 604H501.

surface is 70 m. The total volume of the landslide mass is approximately  $1.2 \times 10^7 \text{ m}^3$ , which is a huge landslide mass.

### 3.2. Basic characteristics of landslide dams

The dammed lake below the Taixianhe 1# landslide mass is 19 m wide, 35 m from the gully head, 123 m long, and approximately 2400 m<sup>2</sup> in total area. The PDL deposit is characterized as earthy yellow, powdery, and lacustrine. The shallow pit is circular, with a diameter of 1.0 m and a depth of 1.1 m. It is fine powder with a depth of 0–50 cm, no sand particles, high humidity, water accumulation, and no bedding. A calcareous nodule with a diameter of 10 cm is observed at a depth of 80 cm. A piece of a calcareous nodule with a diameter of 20 cm and several calcareous nodules with a diameter of 3–5 cm are observed at a depth of 90 cm.

The landslide dam below the Taixianhe 2# landslide mass is 54 m wide, and there is a bifurcation 96 m from the gully head. The north bifurcation is 19 m wide and 88 m long, and the south bifurcation is 23 m wide and 81 m long, with a total area of approximately 7550 m<sup>2</sup>. To sample the shallow pit, the pit mouth was a 100 cm × 50 cm rectangle with a depth of 120 cm. The overall characteristics of the deposit are yellowish-brown, powdery, and lacustrine. The 0–50 cm depth is lacustrine sedimentary clay, light brown-yellow. Calcareous nodules of various shapes appeared at a depth of 60 cm, one of which was a cylindrical nodule with a length of 14 cm and an elliptical cross-section of 5 cm × 4 cm; the other was a corner-shaped nodule, and various shapes of calcareous nodules appeared at 60–80 cm depth, and the largest triaxial was 15 cm × 10 cm × 5 cm. The shallow pit depth was 90 cm, and the shape changed to a 50 × 50 cm square section, mainly clay.

The maximum width of the landslide dam below the Taixianhe 3# landslide mass is 92 m, gradually narrowing toward the gully head, with a total length of 396 m and a total area of approximately 28000 m<sup>2</sup>. The landslide dam has an obvious embankment slope, and the front edge of the lake collapses to form a gully. The shallow pit is located 112 m from the dam to the gully head. 100 cm for pithead 1 × 50 cm rectangle with a total depth of 120 cm. At a depth of 45 cm, the shape becomes a 75 cm × 50 cm rectangle, and the shape of the pit bottom becomes a 20 cm × 50 cm rectangle. The PDL deposits are 0–50 cm deep, and calcareous nodules appear at 60 cm deep. A nodule 60–80 cm deep is combined with the PDL deposit, mostly 10 cm × 7 cm × 4 cm, the largest being 18 cm × 12 cm × 11 cm with a near ellipsoidal shape. There was no evidence of tuberculosis at depth of 80–120 cm.

The landslide dam below the Mingti Village landslide is 330 m long in the north-south direction, 150 m wide on the northernmost side, 120 m wide in the middle, and smaller in the south, extending into two fork ditches. The total volume of the PDL deposits is approximately  $1.0 \times 10^4 \text{ m}^3$ , and the surface area of the main body of the landslide dam plus the bifurcated ditch is approximately 80 mu of cultivated land, with corn planted. Based on the actual situation in the field, the gully on the north side of the landslide dam had a large drop of >100 m vertically, showing strong downward erosion, resulting in an erosion depression on the front edge of the landslide dam, that is, the front edge of the landslide mass. The rainwater formed by the current rainfall is mainly discharged from the

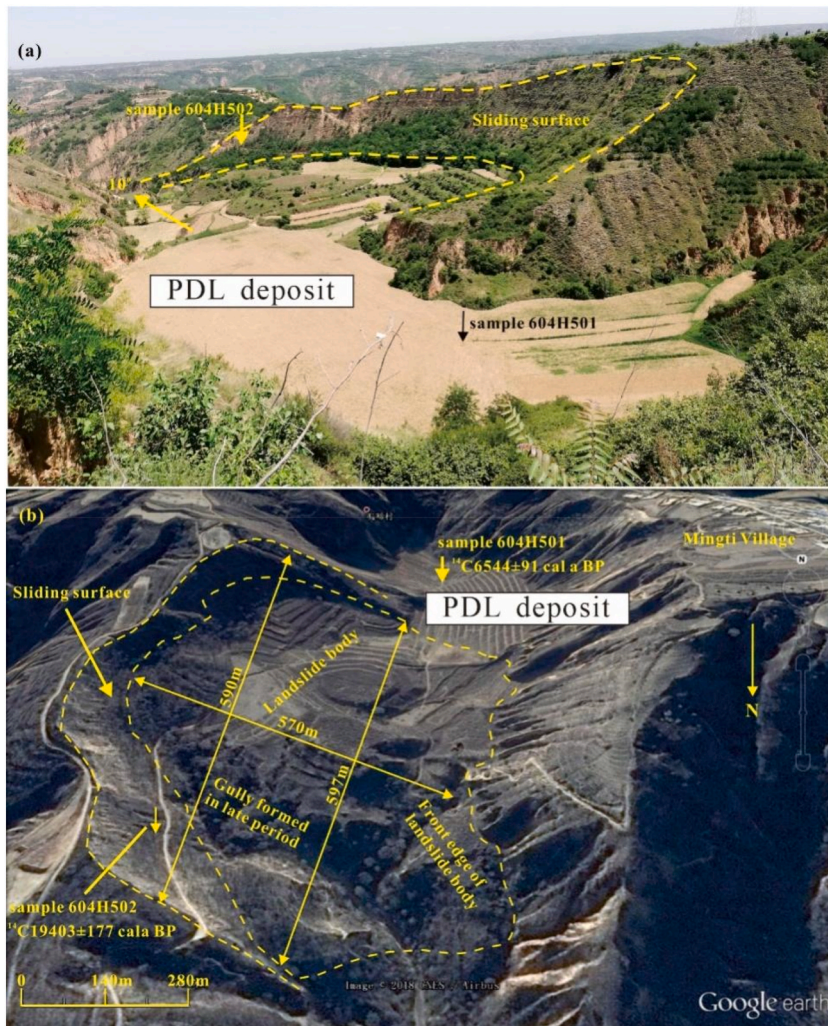


**Fig. 8.** (a) The photo of the Mingti landslide and the landslide dam. (b) The remote sensing images of the Mingti landslide and the landslide dam. gullies in the north, partially absorbed by the cultivated land in the south, and the remainder flows northward along the gullies.

### 3.3. Results and analysis from Carbon-14 dating

All tests were completed using four NEC accelerator mass spectrometers and four isotope ratio mass spectrometers (Thermo Fisher Scientific, Waltham, MA, USA) in a BETA laboratory. “Conventional radiocarbon age” is calculated using Libby half-life, corrected by total fractionation effect, and used for Gregorian calendar age correction. The precision of this age is 10 years, and the unit is BP. When

**Table 1**  
The AMS<sup>14</sup>C dating results of the landslides.

Location	No.	Material	$\delta^{13}\text{C}$ (‰)	Age/cal a BP
Taixianhe 1# landslide	529H101	PDL deposits of the landslide dam	-22.9	3742 ± 95
	529H102	PDL deposits under the landslide dam	-20.8	2748 ± 27
Taixianhe 2# landslide	531H201	PDL deposits of the landslide dam	-21.9	4115 ± 121
	531H202	deposits under the sliding zone	-19.8	13215 ± 91
Taixianhe 3# landslide	601H301	PDL deposits of the landslide dam	-20.2	7814 ± 109
	601H302	deposits under the sliding zone	-20.2	16032 ± 183
Taixianhe 4# landslide	603H401	deposits under the sliding zone	-20.7	8245 ± 79
	603H402	deposits under the sliding zone	-20.0	4470 ± 54
Mingti landslide	604H501	PDL deposits of the landslide dam	-19.1	6544 ± 91
	604H502	deposits under the sliding zone	-20.0	19403 ± 177

the result is greater than the modern reference standard, it is reported as the percentage of the modern carbon content. This modern reference standard is 95% of 14 in NISTSRM-4990C (oxalic acid). The use error is 1 sigma standard deviation. When the statistical standard deviation (sigma) is less than  $\pm 30$  years,  $\pm 30$  BP will be conservatively used as the standard deviation. Table 1 lists the  $^{14}\text{C}$  dating data.

This study strictly determined the thickness and depth of the PDL deposits of a landslide dam during sample collection to ensure the reliability of the sample age. The four age samples of the landslide dams in this study represent the age of the formation of four landslides, that is, the median age of  $^{14}\text{C}$  calibration is  $3742 \pm 95$ ,  $4115 \pm 121$ ,  $7814 \pm 109$ , and  $6544 \pm 91$  cal a BP.

For the 4# landslide mass in Taixianhe Village, the original sliding surface was scoured to form secondary deposits under rainfall conditions, with ages of  $4470 \pm 54$  and  $8245 \pm 79$  cal a BP, which represent two heavy rainfall events. Due to the small volume of the 1# landslide mass in Taixianhe Village, the  $2748 \pm 27$  cal a BP age below the sliding surface represents the age of deposit formed by rain washing the sliding surface after the formation of the landslide mass. For Taixianhe Village 2#, Taixianhe Village 3#, and Mingti Village landslide masses, the landslide mass volume was relatively large. The ages obtained below the sliding surface were  $13215 \pm 91$ ,  $16032 \pm 183$ ,  $19403 \pm 177$  cal a BP, which was older than the age of the PDF deposits of landslide dam. Whether this reflects the age of the original stratum or other events before the landslide mass was formed requires further investigation.

#### 4. Mechanism for old landslides and landslide dam

From deposit sampling of the dammed lake under the 1–3# landslide masses of the Taixian River, calcareous nodules of different shapes and sizes were found in PDL deposits. The nodules do not have the characteristics of the original deposit sequence but are washed, transported, and deposited into the dammed lake by the surface water formed during rainfall. Under rainfall conditions, the landslide mass blocks the valley, and a landslide dam forms. The previous deposits mainly originated from loose material on either side of the valley. With continuous rainfall, the calcareous nodules on the surrounding surface are transported and deposited. The characteristics of the lacustrine profile show that the sampling location is reasonable for this research; alternatively, the composition of landslide mass, landslide dam, and PDL deposits shows that this is a heavy rainfall process in the area, not a slight one.

For the Taixianhe 4# landslide mass, the landform and the characteristics of multiple rainwater gullies on the sliding surface showed that the landslide mass, as an ancient or old landslide mass, is planned to be formed at a scale of ten thousand years. The unconformity boundary between the modern deposit and the original stratum was very evident. In the secondary deposit profile formed by heavy rainfall scouring the original sliding and surrounding surfaces, there are nodules of various shapes and alluvial–proluvial gravel of various sizes. The age of sample 603H401 is  $8245 \pm 79$  cal a BP, representing the heavy rainfall process in this period. On the right side of the original slip surface, during rainfall, the deposits subsided and were deposited again, with a total thickness of 120 cm and a depth of 80 cm, and nodules were observed. The 603H402 samples were collected from the bottom of the nodules. This type of deposit is in unconformable contact with the N2 Red Lake deposits. The obtained age is  $4470 \pm 54$  cal a BP, representing another rainfall process.

Since the Holocene, there has been little rainfall in the Loess Plateau [28,32]. For occasional long-term rainfall, the rainfall exceeded the critical value, and the weight and stress fields of the loess changed. The original landform changed after the landslide formation. For local areas of the Loess Plateau, sudden super-heavy rainfall far exceeded that of adjacent areas. The aforementioned rainfall event in October 2021 in Daning County, Shanxi Province, is a sudden formation in the dynamic process of gravity “collapse” of the valley without perennial water. Unlike valleys with perennial water, lateral erosion and transportation of the river accumulate and form over a long period.

In addition to heavy rainfall, the formation causes of landslide dams also include the following aspects: first, the inclination of the original loess slope is  $> 60^\circ$ : For Taixianhe 1, 2, 3, and 4# landslides, the inclinations of the back wall of the sliding surface are  $90^\circ$ ,  $90^\circ$ ,  $85^\circ$ , and  $80^\circ$  respectively, and the inclination of the sliding surface of Mingti Village landslide is  $70^\circ$ . Before the landslide was formed, the inclination of the original loess slope surface was  $> 60^\circ$ . Rainwater formed by heavy rainfall quickly converged into the valley and flowed down along the valley, removing a large quantity of loose deposits from the original trunk ditch. Under the action of gravity, the high angle slope “collapsed” and “slid,” causing the landslide. This is the dynamic mechanism of the large inclination of the back wall of the sliding surface formed by this landslide. Second, the geomorphic characteristics of the valley determine the formation of landslide dams: the geomorphic form of the original valley is a “V” shape. The larger the slope angle of the rainfall water in the valley, the longer the distance from the entire valley to the main riverbed, which facilitates the formation of a landslide dam. However, it is difficult to form a landslide dam in the open valley with a “U” shape close to the gully head. For gullies of the same shape, the greater the intensity of rainfall, the larger the scale of the landslide mass, and the larger the range of the landslide dam.

#### 5. Discussion

Multiple flood events have occurred in the Loess Plateau since the Holocene [28,33], which have caused ancient landslides. However, because of climate change, extreme rainfall events may be even more frequent today than in the past [34,35]. For example, the strongest rainfall event was recorded in Daning County in October 2021 based on meteorological records. Hence, it is highly likely that these ancient landslides will be activated in a certain time of the future. In this study, the Taixian River area in Daning County was considered a landslide-prone area because ancient landslide groups and landslide dams were observed. Detailed field investigations and remote sensing images contributed to the determination of this point. Hence, it is essential to improve disaster prevention and management to reduce direct and indirect losses caused by sudden heavy rainfall events in this region. For this purpose, the implementation of in-situ monitoring and early warning systems may be helpful tools, and they have proven efficient in the practice of

landslide risk reduction in China [36,37]. For other places in the study area, the safety of villages and infrastructure, particularly those near loess geomorphic units and slopes with large slope angles, should be given more attention.

Two main factors have triggered ancient landslides in the Loess Plateau: monsoon rainfall and tectonic activities, including earthquakes. In this study, it is evident that earthquakes may be a potential triggering factor because this region is highly seismic and includes several large strike-slip faults. Relevant cases have been reported in the literature revealing the important role of faults and earthquakes in this region [8,38,39]. However, no evidence revealing the role of the earthquake during the landslide occurrence in our case was observed, including, but not limited to, that of drilling and geomagnetism. In contrast, the  $^{14}\text{C}$  dating results showed a difference in the age of the landslide and PDL deposits of the landslide dams. Therefore, heavy rainfall events may be more likely to trigger landslides in this study, and more than one rainfall event influenced the landslide group during its occurrence and development. However, this point is still a source for the uncertainty in our study, hence it is important not to avoid it. Future geophysical survey data may be helpful in obtaining more evidence to determine the specific role of earthquakes in these landslides, which was lacking in this study. In addition, geophysical survey data can provide an accurate stratigraphic column of deposits to better capture the basic characteristics of PDL deposits.

## 6. Conclusions

- (1) During the Holocene (2700, 3700–4400, 6500, and 7800–8200 years ago), heavy rainfall was the main cause of landslide and landslide dam formation in the Loess Plateau.
- (2) Under the condition of heavy rainfall in Daning County, the slopes with slope angles  $>60^\circ$  are prone to developing mass movements, including landslides. The scale of the landslide is related to the rainfall intensity. When the sliding direction is perpendicular to the valley direction, a landslide dam can easily occur, and it is difficult to form a landslide dam if the sliding direction is close to the valley direction.
- (3) Giant ancient landslides triggered by heavy rainfall normally began with the sudden collapse or sliding of loess geological masses. During this process, the formation and size of landslide dams were determined by the landform of the original valley, rainfall intensity, and scale and sliding direction of the landslide mass.

## Author contribution statement

Zhenming Zhao: Conceived and designed the experiments; Performed the experiments; Contributed reagents, materials, analysis tools or data; Wrote the paper.

Yaming Tang: Conceived and designed the experiments; Analyzed and interpreted the data; Wrote the paper.

Fan Feng: Performed the experiments; Analyzed and interpreted the data; Contributed reagents, materials, analysis tools or data.

Zhengguo Li: Conceived and designed the experiments; Contributed reagents, materials, analysis tools or data; Wrote the paper.

Yong Xu: Performed the experiments; Contributed reagents, materials, analysis tools or data.

Bo Hong: Analyzed and interpreted the data.

Wei Feng: Contributed reagents, materials, analysis tools or data.

## Data availability statement

Data will be made available on request.

## Declaration of competing interest

The authors declare that they have no known competing financial interests or personal relationships that could have appeared to influence the work reported in this paper.

## Acknowledgements

The research was supported by the Technology Innovation Team Project of Shaanxi Province: Innovation Team for geohazard risk prevention and controlling based on IT technology (2023-CX-TD-33), and the Key Research & Development Project of Shaanxi Province: Research and application of key technologies for geohazard mechanism and risk assessment based on big data (2019ZDLSF07-07-02).

## References

- [1] D.N. Petley, Global patterns of loss of life from landslides, *Geology* 40 (2012) 927–930.
- [2] R. Emberson, D. Kirschbaum, T. Stanley, Global connections between El Nino and landslide impacts, *Nat. Commun.* 12 (2021) 2262.
- [3] Z. Guo, O. Torra, M. Hürlimann, V. Medina, Polo Puig, C. Fslam, A QGIS plugin for fast regional susceptibility assessment of rainfall-induced landslides, *Environ. Model. Software* 150 (2022), 105354.
- [4] Z. Li, F. Zheng, W. Liu, D.C. Flanagan, Spatial distribution and temporal trends of extreme temperature and precipitation events on the Loess Plateau of China during 1961–2007, *Quat. Int.* 226 (1–2) (2010) 92–100.

- [5] J. Zhuang, J. Peng, G. Wang, I. Javed, Y. Wang, W. Li, Distribution and characteristics of landslide in Loess Plateau: a case study in Shaanxi province, *Eng. Geol.* 236 (2018) 89–96.
- [6] Y. Tang, Z. Guo, L. Wu, B. Hong, W. Feng, X. Su, Z. Li, Y. Zhu, Assessing debris flow risk at a catchment scale for an economic decision based on the LiDAR DEM and numerical simulation, *Front. Earth Sci.* 10 (2022), 821735.
- [7] Z. Guo, B. Tian, G. Li, D. Huang, T. Zeng, J. He, D. Song, Landslide susceptibility mapping in the Loess Plateau of northwest China using three data-driven techniques—a case study from middle Yellow River catchment, *Front. Earth Sci.* 10 (2023), 1033085.
- [8] J. Peng, Z. Fan, D. Wu, J. Zhuang, F. Dai, W. Chen, C. Zhao, Heavy rainfall triggered loess-mudstone landslide and subsequent debris flow in Tianshui, China, *Eng. Geol.* 186 (2015) 79–90.
- [9] K. Zheng, J.Z. Wei, J.Y. Pei, H. Cheng, X.L. Zhang, F.Q. Huang, F.M. Li, J.S. Ye, Impacts of climate change and human activities on grassland vegetation variation in the Chinese Loess Plateau, *Sci. Total Environ.* 660 (2019) 236–244.
- [10] J. Zhuang, J. Peng, C. Xu, Z. Li, A. Densmore, D. Milledge, J. Iqbal, Y. Cui, Distribution and characteristics of loess landslides triggered by the 1920 Haiyuan Earthquake, Northwest of China, *Geomorphology* 314 (2018) 1–12.
- [11] M. Zhang, J. Liu, Controlling factors of loess landslides in western China, *Environ. Earth Sci.* 59 (2010) 1671–1680.
- [12] F.C. Dai, C.F. Lee, Y.Y. Ngai, Landslide risk assessment and management: an overview, *Eng. Geol.* 64 (1) (2002) 65–87.
- [13] Z. Guo, L. Chen, K. Yin, D.P. Shrestha, L. Zhang, Quantitative risk assessment of slow-moving landslides from the viewpoint of decision-making: a case study of the Three Gorges Reservoir in China, *Eng. Geol.* 273 (2020), 105667.
- [14] Q. Zhou, Q. Xu, D. Peng, X. Fan, C. Ouyang, K. Zhao, H. Li, X. Zhu, Quantitative spatial distribution model of site-specific loess landslides on the Heifangtai terrace, China, *Landslides* 18 (2021) 1163–1176.
- [15] J.M. Dortch, L.A. Owen, W.C. Haneberg, M.W. Caffee, C. Dietsch, U. Kamp, Nature and timing of large landslides in the Himalaya and Transhimalaya of northern India, *Quat. Sci. Rev.* 28 (11–12) (2009) 1037–1054.
- [16] H. Qiu, Y. Cui, S. Hu, D. Yang, Y. Pei, S. Ma, Z. Liu, Size distribution and size of loess slides in response to slope height and slope gradient based on field survey data, *Geomatics, Nat. Hazards Risk* 10 (1) (2019) 1443–1458.
- [17] L. Wang, S. Shao, F. She, A new method for evaluating loess collapsibility and its application, *Eng. Geol.* 264 (2020), 105376.
- [18] Y. Tang, F. Feng, Z. Guo, W. Feng, Z. Li, J. Wang, Q. Sun, H. Ma, Y. Li, Integrating principal component analysis with statistically-based models for analysis of causal factors and landslide susceptibility mapping: a comparative study from the loess plateau area in Shanxi (China), *J. Clean. Prod.* 277 (2020), 124159.
- [19] V. Medina, M. Hürlimann, Z. Guo, A. Lloret, J. Vaunat, Fast physically-based model for rainfall-induced landslide susceptibility assessment at regional scale, *Catena* 201 (2021), 105213.
- [20] F. Chen, Q. Xu, J. Chen, H.J.B. Birks, J. Liu, S. Zhang, L. Jin, C. An, R.J. Telford, X. Cao, Z. Wang, X. Zhang, K. Selvaraj, H. Lu, Y. Li, Z. Zheng, H. Wang, A. Zhou, G. Dong, J. Zhang, X. Huang, J. Bloemendal, Z. Rao, East Asian summer monsoon precipitation variability since the last deglaciation, *Sci. Rep.* 5 (2015), 11186.
- [21] J. Dong, C.C. Shen, X. Kong, C.C. Wu, H.M. Hu, H. Ren, Y. Wang, Rapid retreat of the East Asian summer monsoon in the middle Holocene and a millennial weak monsoon interval at 9 ka in northern China, *J. Asian Earth Sci.* 151 (2018) 31–39.
- [22] J. Cao, Z. Rao, F. Shi, E. Lian, G. Jia, Lake-level records support a mid-Holocene maximum precipitation in northern China, *Sci. China Earth Sci.* 64 (12) (2021) 2161–2171.
- [23] P.A. Mayewski, E.E. Rohling, J. Curt Stager, W. Karlén, K.A. Maasch, L. David Meeker, E.A. Meyerson, F. Gasse, S. van Kreveld, K. Holmgren, J. Lee-Thorp, G. Rosqvist, F. Rack, M. Staubwasser, R.R. Schneider, E.J. Steig, Holocene climate variability, *Quat. Res.* 62 (3) (2004) 243–255.
- [24] S. Hu, H. Qiu, N. Wang, X. Wang, S. Ma, D. Yang, N. We, Z. Liu, Y. Shen, M. Cao, Z. Song, Movement process, geomorphological changes, and influencing factors of a reactivated loess landslide on the right bank of the middle of the Yellow River, China, *Landslides* 19 (2022) 1265–1295.
- [25] Z. Guo, J.V. Ferrer, M. Hürlimann, V. Medina, C. Puig-Polo, K. Yin, D. Huang, Shallow landslide susceptibility assessment under future climate and land cover changes: a case study from southwest China, *Geosci. Front.* 14 (4) (2023), 101542.
- [26] Z. Guo, B. Tian, J. He, C. Xu, T. Zeng, Y. Zhu, Hazard assessment for regional typhoon-triggered landslides by using physically-based model -A case study from southeastern China, *Georisk* (2023), <https://doi.org/10.1080/17499518.2023.2188465>.
- [27] G. Cheng, L. Guo, T. Zhao, J. Han, H. Li, J. Fang, Automatic landslide detection from remote-sensing imagery using a scene classification method based on BoVW and pLSA, *Int. J. Rem. Sens.* 34 (1) (2013) 45–59.
- [28] T. Stevens, D.S.G. Thomas, S.J. Armitage, H.R. Lunn, H. Lu, Reinterpreting climate proxy records from late Quaternary Chinese loess: a detailed OSL investigation, *Earth Sci. Rev.* 80 (1–2) (2007) 111–136.
- [29] M. Delchiaro, G. Iacobucci, F. Troiani, M.D. Seta, P. Ballato, L. Aldega, Morphoevolution of the Seymareh landslide-dam lake system (Zagros Mountains, Iran): implications for Holocene climate and environmental changes, *Geomorphology* 413 (2022), 108367.
- [30] G. Ha, F. Liu, M. Cai, J. Pei, X. Yao, L. Li, Radiocarbon dating of the nyixoi chongco rock avalanche, southern tibet: search for signals of seismic shaking and hydroclimatic events, *Front. Earth Sci.* 9 (2021), 793460.
- [31] Z. Yuan, J. Chen, L.A. Owen, K.A. Hedrick, M.W. Caffee, W. Li, L.M. Schoenbohm, A.C. Robinson, Nature and timing of large landslides within an active orogen, eastern Pamir, China, *Geomorphology* 182 (2013) 49–65.
- [32] L.Y. Xiong, S.J. Li, G.H. Hu, K. Wang, M. Chen, A.X. Zhu, G.A. Tang, Past rainfall-driven erosion on the Chinese loess plateau inferred from archaeological evidence from Wucheng City, Shanxi, *Communications Earth & Environment* 4 (2023) 4.
- [33] H. Lu, X. Wang, Y. Wang, X. Zhang, S. Yi, X. Wang, T. Stevens, R. Kurbanov, S.B. Marković, Chinese loess and the Asian monsoon: what we know and what remains unknown, *Quat. Int.* 620 (2022) 85–97.
- [34] S.L. Gariano, F. Guzzetti, Landslides in a changing climate, *Earth Sci. Rev.* 162 (2016) 227–252.
- [35] M. Hürlimann, Z. Guo, C. Puig-Polo, V. Medina, Impacts of future climate and land cover changes on landslide susceptibility: regional scale modelling in the Val d’ Aran region (Pyrenees, Spain), *Landslides* 19 (2022) 99–118.
- [36] Y. Yin, H. Wang, Y. Gao, X. Li, Real-time monitoring and early warning of landslides at relocated wushan town, the three gorges reservoir, China, *Landslides* 7 (2010) 339–349.
- [37] X. Wang, K. Wang, F. Lin, K. Guo, Preliminary report on the landslide early warning on august 20, 2021, in nangqian county, Qinghai province, China, *Sci. Rep.* 12 (2022) 9795.
- [38] W. Fan, J. Lv, Y. Cao, M. Shen, L. Deng, Y. Wei, Characteristics and block kinematics of a fault-related landslide in the Qinba Mountains, western China, *Engineering Geology* 249 (2019) 162–171.
- [39] C. Liang, H. Zhang, T. Wang, Red clay/mudstone distribution, properties and loess–mudstone landslides in the Loess Plateau, China, *Environ. Earth Sci.* 81 (2022) 386.